Available online at www.sciencedirect.com
ScienceDirect
Cement and Concrete Research 37 (2007) 559–564
Cement and Concrete Research

Use of limestone obtained from waste of the mussel cannery industry for the production of mortars

Paloma Ballester [a], Isabel Mármol [a], Julián Morales [b], Luis Sánchez [b,*]

[a] Cementos Kola S.A. (CEMKOSA), Avda. Agrupación Córdoba no. 17, Córdoba, Spain
[b] Departamento de Química Inorgánica, Facultad de Ciencias — Universidad de Córdoba, Campus de Rabanales, Edificio Marie Curie, 14071, Córdoba, Spain

Received 8 March 2006; accepted 11 January 2007

Abstract

Various types of cement−SiO_2−$CaCO_3$ mortar were prepared by replacing quarry limestone aggregate with limestone obtained as a by-product from waste of the mussel cannery industry. The $CaCO_3$ aggregate consists mainly of elongated prismatic particles less than 4 μm long rather than of the rounded particles of smaller size (2–6 μm) obtained with quarry limestone. The mechanical and structural properties of the mortars were found to be influenced by aggregate morphology. Setting of the different types of mortar after variable curing times was evaluated by scanning electron microscopy (SEM), thermogravimetric analysis (TG) and mercury intrusion porosimetry (MIP) techniques. Mortars with a high content in mussel shell limestone exhibited a more packed microstructure, which facilitates setting of cement and results in improved mortar strength. The enhanced mechanical properties of the new mortars allow the cement content in the final mortar composition to be decreased and production costs to be reduced as a result.

Keywords: Mortar; Limestone; Waste management; Mechanical properties; Thermal analysis

1. Introduction

Dry mortars generally contain at least three components, namely: a binder, an aggregate and additives [1]. New mortar formulations are continuously developed where the incorporation of new components (additives mainly) enhances mechanical properties such as strength, durability, rheological behaviour or workability. Also, they reduce production costs in some cases. Cement, which is the binder element in mortar, is one of the most expensive components; therefore, its partial replacement is an attractive way of reducing production costs provided mechanical properties are preserved or even improved.

The vast amounts of industrial waste produced at present make their disposal or processing a major challenge. The use of industrial waste in admixtures for the production of structural materials has helped alleviate this problem. Thus, it not only reduces energy consumption in the production of structural materials by partially replacing cement, but also contributes to environmental protection. Recently, various waste materials including construction rubble [2], tire rubber ash [3], blag furnace slag [4] silica fume [5] and fly ash [6] have been tested in the preparation of dry mortars with proven advantages and its beneficial reported. Most of the new binder/aggregate admixtures improve the mechanical properties of mortar and allow the proportion of cement content in the mortar composition to be reduced.

In this work, limestone obtained from mussel shell waste of the cannery industry was used as a new filler material to produce mortar. The industry managing the reuse and recycling of mussel shell waste has become a major source of limestone. Thus, more than 80 000 tonnes of limestone per year are generated in Galicia, a northwestern region where the cannery industry is very important. Quartz−limestone−dolomite mixtures are widely used as aggregates. The binder/aggregate ratio and aggregate characteristics (*viz*. grain size distribution, chemical composition and particle shape) alter the workability and mechanical properties of mortar [7]. An appropriate choice of aggregates can provide new formulations for high performance mortars. The limestone used in this work possesses a special particle morphology departing from that typical of quarry limestone. Based on the experimental results reported

* Corresponding author. Tel.: +34 957 218620; fax: +34 957 218621.
E-mail address: luis-sanchez@uco.es (L. Sánchez).

0008-8846/$ - see front matter © 2007 Elsevier Ltd. All rights reserved.
doi:10.1016/j.cemconres.2007.01.004

Table 1
Percent oxide composition, density and specific area of Portland cement CEM II/A-V 42.5 R

SiO_2	26.96
Al_2O_3	9.65
Fe_2O_3	3.43
CaO	54.07
MgO	1.41
SO_3	3.22
K_2O	1.40
CaO free	1.03
Density (g/cm^3)	2.96
Specific surface (Blaine) (m^2/kg)	360

here, replacing ordinary limestone with limestone obtained from mussel shells improves the physico-mechanical properties of the resulting mortar.

2. Experimental

The mortars were prepared from cement, natural silica sand and limestone. The cement was of the Portland CEM II/A-V 42.5R type. Its composition and fineness are shown in Table 1. The SiO_2 used was of controlled grain size, with at least 90% of particles less than 500 μm. The limestone, (hereafter named q-limestone), was obtained from a quarry in Fuentes de Andalucía (Spain); it was a fine aggregate containing more than 98% $CaCO_3$. The limestone obtained from mussel shells, which was manufactured by *Calizamar S.A.* and is hereafter named m-limestone, was converting pristine waste of the mussel cannery industry in the following three steps: (i) washing process to remove salt components from sea shells, followed by (ii) heating at a high temperature to remove water and organic materials, and (iii) grinding of the calcined product. Chemical analysis revealed the following composition: 96% $CaCO_3$, 1.12% $CaMg(CO_3)_2$, <0.1% NaCl, 95 ppm Fe_2O_3 and minor impurities. Two types of mortar were prepared. One was obtained simply by replacing q-limestone with m-limestone and maintaining the cement and silica contents (samples A to D). In the other, q-limestone was completely replaced with m-limestone, and so was some cement (samples E and F). The purpose of this latter test was to check whether the new component would allow the production of mortars with a somewhat lower cement content while maintaining the mechanical properties of the original material and reducing its manufacturing cost. The composition of the six samples is shown in Table 2.

A water/mortar ratio of 0.16 resulted in appropriate consistency and acceptable workability. All samples were cured at 25 °C and 50−90% relative humidity (RH). Compressive and flexural strength tests [UNE-EN 1015-11] were performed on prismatic specimens of size 40×40×160 mm that were examined after 24 h, 7, 28 and 90 days of curing. Adhesion tests were done on the prewetted surface of 30×30×4 cm bricks [UNE-EN 1015-12]. Consistency was determined using the flow table test [UNE-EN 1015-3].

Table 2
Percent composition of the mortars studied

Component	Sample A	Sample B	Sample C	Sample D	Sample E	Sample F
Cement	10	10	10	10	9.5	9
SiO_2	78	78	78	78	78	78
q-$CaCO_3$	12	8	4	–	–	–
m-$CaCO_3$	–	4	8	12	12.5	13

Pore size distribution was determined with a Fisons Instruments 2000 mercury porosimeter after 28 days of curing. For these measurements, samples were placed in a desiccator coupled to a vacuum pump in order to remove moisture until weight constancy was reached. Scanning electron microscopy (SEM) images were obtained with a Jeol JMS-6400 microscope. Particle size distributions were determined with a laser analyzer (Mastersizers S, Malvern, UK). Thermogravimetric analysis (TG) was done with a CAHN 2000 thermobalance, heating from 25 to 850 °C at a rate of 5 °C min^{-1} under ambient conditions. The final temperature was held for 1 h.

3. Results and discussion

For easier understanding, this section begins with a description of the properties of samples A−D, where a fraction of q-limestone was replaced with m-limestone. Fig. 1 illustrates the influence of aggregates on the compressive and flexural strength of the mortars after variable curing times. All measurements were made in triplicate in order to ensure reliability in the results of the mechanical tests. The calculated standard

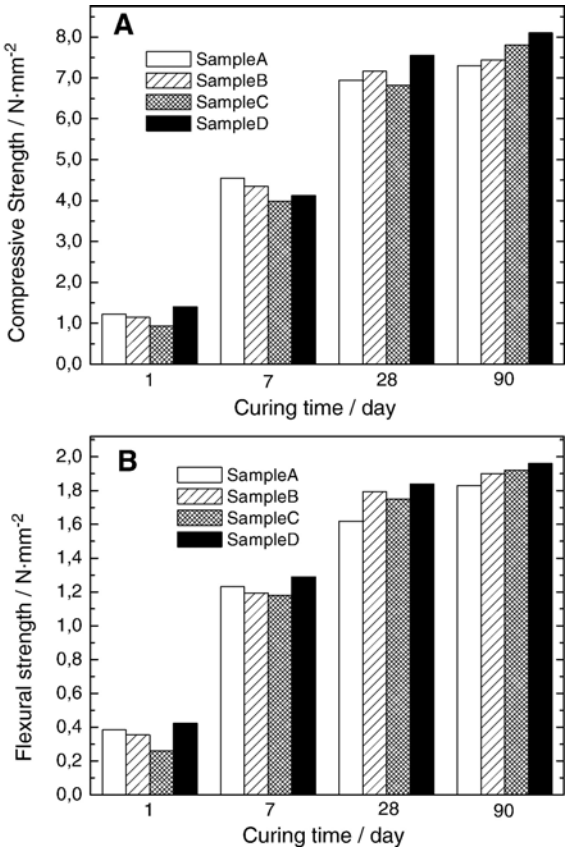

Fig. 1. (A) Compressive and (B) flexural strength as a function of curing time in mortars prepared by replacing q-$CaCO_3$ with m-$CaCO_3$.

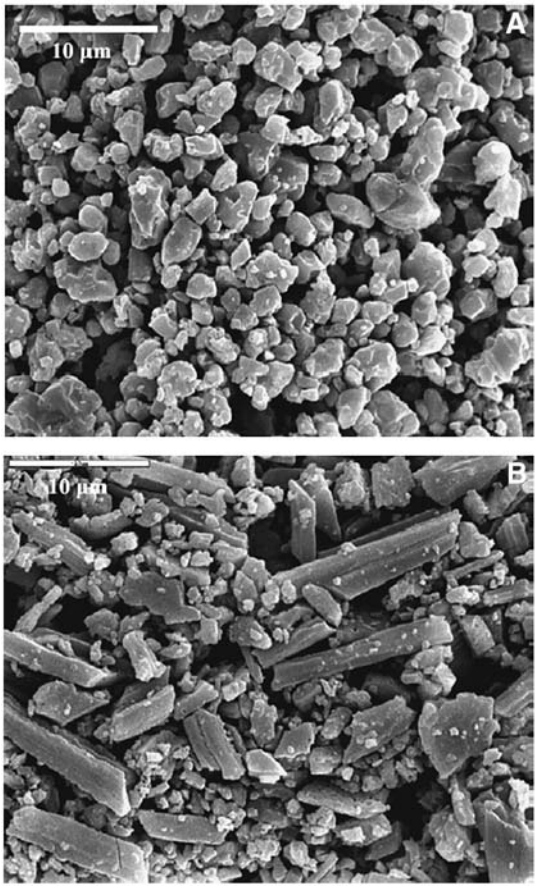

Fig. 2. SEM images of the limestone aggregates: (A) q-$CaCO_3$ and (B) m-$CaCO_3$.

deviation was less than 3%. Therefore, the differences between samples A and D at any given age were significant. As expected, the strength values increased with curing time. At an early stage of curing (up to day 7) the mortars reached around 50% of their maximum strength. Such strength resulted from hydration of the cementitious phases in mortar to form hydrated calcium silicates (commonly CSH phases), as major compounds. At short curing times (up to 7 days), mortar strength decreased as the m-limestone content increased; by exception, the strength of sample D was somewhat higher than that of sample A. At longer curing times, the opposite behavior was observed: compressive and flexural strength increased with increasing m-limestone content. Bearing in mind the chemical composition of m-limestone, no pozzolanic activity was to be expected from its components. Therefore, increased strength at long curing times must have arisen from differences in internal microstructure and/or the kinetics of the setting process.

Fig. 2 shows selected SEM images of the two $CaCO_3$ aggregates used to prepare the mortars. Whereas q-limestone exhibited rounded particles of size ranging from 2 to 6 μm (Fig. 2A), m-limestone exhibited an assorted morphology consisting mainly of large prismatic particles up to 14 μm in length (Fig. 2B). A small fraction of submicron particles was also observed in both aggregates. Although particle size distribution, Fig. 3, was essentially consistent with the SEM images, there were some differences worth noting. Thus, the

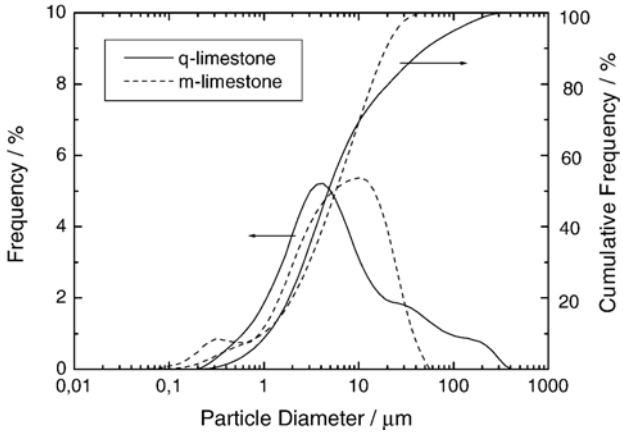

Fig. 3. Particle size distribution of the (a) q-$CaCO_3$ and (b) m-$CaCO_3$.

particle size distribution for q-limestone was multimodally shaped and most particles were around 2 μm in size. The particle size distribution for m-limestone, however, was shaped differently; thus, it appeared as a strong, broad peak the maximum of which was located at *ca.* 10 μm, which is close to the length of the prismatic-shaped particles. A small fraction of particles less than 1 μm in size was also observed, consistent with the small spots present in the SEM images (see Fig. 2B). Intercrossing of particles of *pseudo*-prismatic morphology may

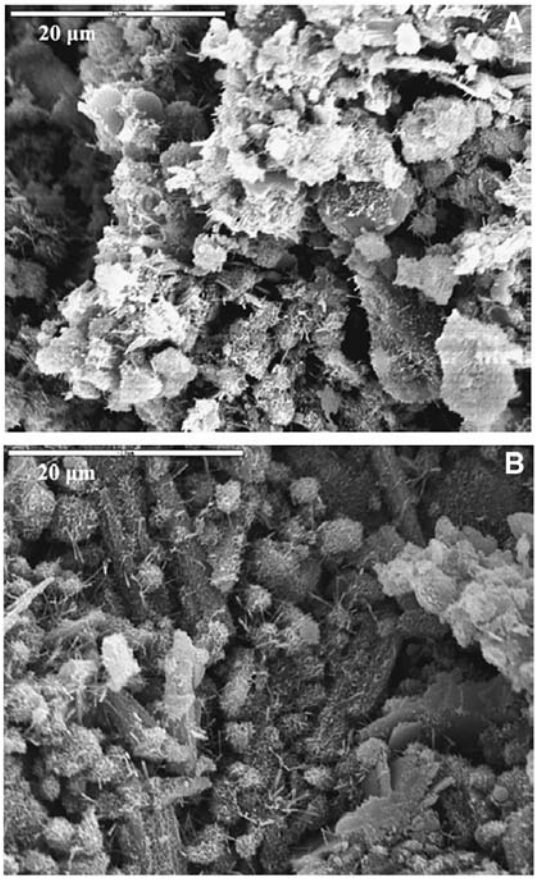

Fig. 4. SEM images of sample A (A) and C (B) after 28 days of curing.

Table 3
Consistency and adhesion strength of the mortars

	Sample A	Sample B	Sample C	Sample D
Consistency/mm	155	157	157	162
Adhesion/N mm^{-2}	0.32	0.43	0.44	0.47

result in the formation of a network where cement particles bind strongly to the aggregates upon solidification of the cement slurry, thus increasing the strength of the mortar. A rounded morphology in the aggregate must hinder formation of this interconnected system [7] that helps bind the different components as cement hydration progresses. This assumption was confirmed by the SEM images for samples A and C after 28 days of curing (Fig. 4), where the microstructure of sample C reflected increased interparticle connectivity and more compact packing. A similar finding (*viz*. improved mechanical strength of lime-based mortars upon crushing) was previously reported by Lanas and Alvarez [8], who ascribed it to improved packing associated with the angular shape adopted by the ground particles.

The difference in grain characteristics between the limestones influenced various physico-mechanical properties of mortar including consistency (defined as the resistance of fresh mortar to undergo deformation, UNE-EN 1015-3). The test involves measuring the increase in diameter of the lower base of a truncated cone of moulded mortar in a cast 6 cm high with an upper and lower diameter of 7 and 10 cm, respectively and the adhesion strength (see Table 3). The spread diameter increased with m-limestone content and ranged from 155 mm for sample A to 162 mm for sample D. Therefore, the mortars containing m-limestone as aggregate were more workable. The water/mortar ratio, initially fixed at 0.16 in all samples, must be increased in sample A in order to obtain similar consistency values [9]. Differences in rheological properties between the limestones associated with their disparate particle morphology may account for the previous results. Thus, the smaller average particle size in the q-$CaCO_3$ aggregate must facilitate water adsorption [10] and detract from mortar workability. Also, the mortars made from m-limestone exhibited higher adhesion strength (Table 3) by virtue of their improved cementation properties.

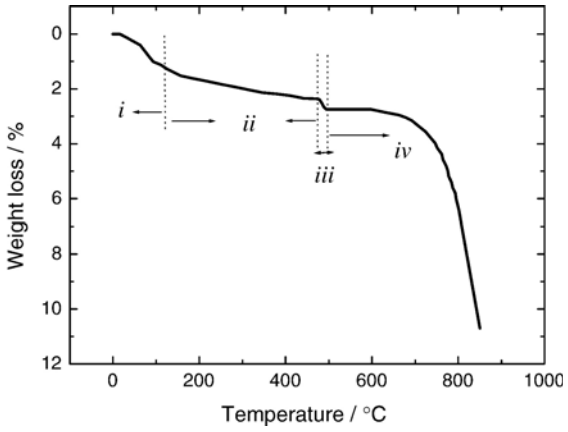

Fig. 5. Thermogravimetric curve for sample A after 7 days of curing.

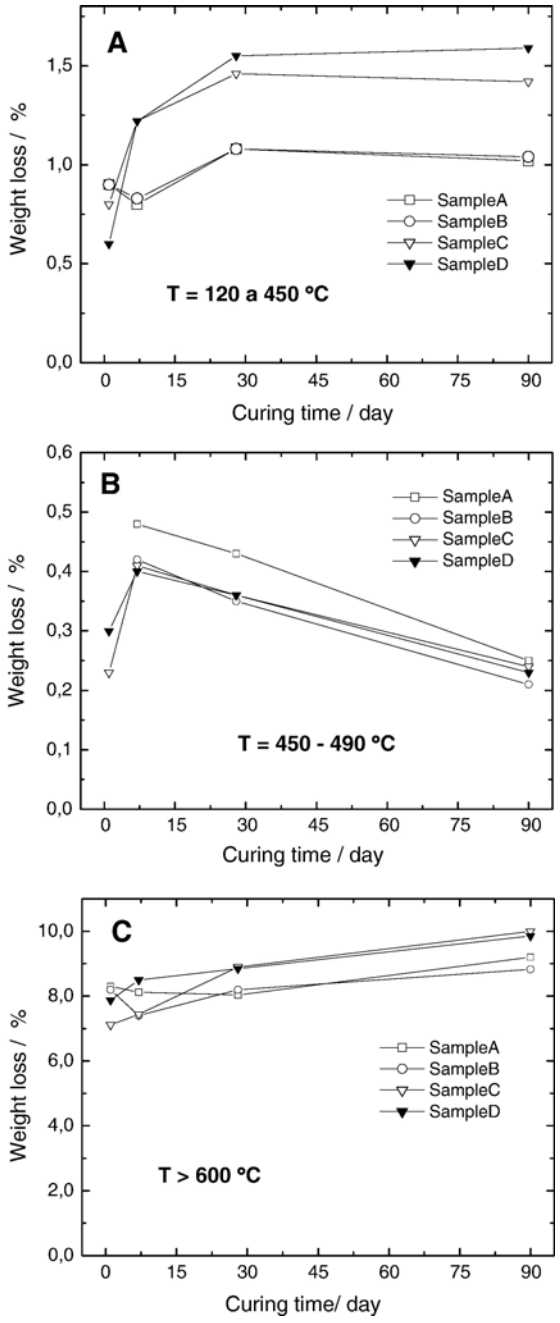

Fig. 6. Weight losses as a function of curing time in various temperature ranges: (A) 120–450 °C, (B) 450–490 °C and (B) >600 °C.

Thermal analysis tests were conducted with a view to interpreting the correlation observed between the limestone aggregates and mortar strength. By way of example, Fig. 5 shows the TG curve obtained for sample A after 7 days of curing. The curve shape, which was similar for all samples at different curing times, exhibited four stages. Temperature ranges and relative weight losses are useful for characterizing these materials [11]. The stages observed are associated with different physico-chemical processes, namely: (i) a weight loss due to adsorbed water (25–120 °C); (ii) the loss of chemically

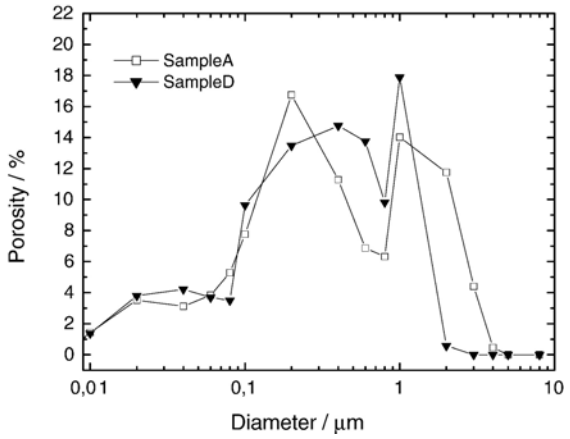

Fig. 7. Pore size distribution of samples A and D after 28 days of curing.

bound water (120–450 °C); (iii) a weight loss associated to dehydroxylation of $Ca(OH)_2$ (450−490 °C) [12]; and (iv) the loss of CO_2 due to the decomposition of carbonates.

A comparison of the weight loss observed in each step of the different curing periods can help one identify the influence of the aggregate on the development of the setting process. Fig. 6 shows the weight losses in the four samples in the three latter stages as a function of curing time. The loss of water from hydrated cementitious phases, mainly CSH (Fig. 6A), tended to increase during the early stages of curing (as expected), and also with increasing m-limestone content — particularly in samples C and D, which were those with the higher contents. Therefore, this aggregate facilitates hydration of calcium silicates, which are responsible for mortar strengthening. Why the amount of hydrated product increases with increasing m-limestone content is unclear. The increased number of nucleation sites in m-limestone relative to q-limestone may provide a plausible explanation in the light of particle size distribution (see Fig. 3). Thus, m-limestone contains a small fraction of particles less than 1 μm in size and its smaller particle size may favor water adsorption, thereby increasing the hydration of cement components. Portlandite, $Ca(OH)_2$, is formed as a by-product of the hydrolysis of calcium silicates according to:

$$SiO_2{\cdot}nCaO + (1.5+n)H_2O \rightarrow SiO_2{\cdot}CaO{\cdot}2.5H_2O + (n-1)Ca(OH)_2; \text{with } n = 2,3 \quad (1)$$

The amount calculated from the weight loss over the range 450−490 °C (Fig. 6B) was greater for sample A − which contained no m-limestone − and decreased on prolonged curing. However, the amount of $Ca(OH)_2$ found was seemingly independent of that of m-limestone added to the mortar. These results can be better understood by considering the weight loss due to limestone decomposition in Fig. 6C. Two features are worth special note, namely (i) in contrast with the results obtained over the range 450−490 °C, the weight loss increased with curing time; (ii) there were substantial differences in weight losses, even though the samples had the same initial limestone content. Again, the greatest weight losses were those from samples C and D, which were those with the highest m-limestone contents. These results are consistent with portlandite formed in reaction (1) undergoing partial carbonation [11] to an extent increasing with increasing m-limestone content.

Some mass balance calculations were done in order to correlate the mass loss of $Ca(OH)_2$ with the mass gain resulting from carbonation. All samples exhibited carbonate gains exceeding the values calculated from the portlandite content — the difference was greater than 100% in some cases. However, not only pure $Ca(OH)_2$, but also the C–S–H system can undergo carbonation — albeit more slowly [13], which hinders the establishment of a direct relationship between the amount of $Ca(OH)_2$ released in reaction (1) and the degree of carbonation from TG data. Nevertheless, the experimental results do demonstrate that m-limestone favors carbonation (from 2.09% as calculated for sample A from 1 to 90 days of curing time to 4.46% as calculated for sample D under the same experimental conditions).

Because $Ca(OH)_2$ forms large crystals that contribute little to mortar strength, its removal should improve the mechanical properties of the mortar. Thus, the combined results of the TG analysis (Fig. 6A−C) expose interesting differences in mortar setting and provide direct evidence that replacing q-limestone with m-limestone increases the rate of hydration and carbonation, thereby increasing the compressive and textural strength of the mortar.

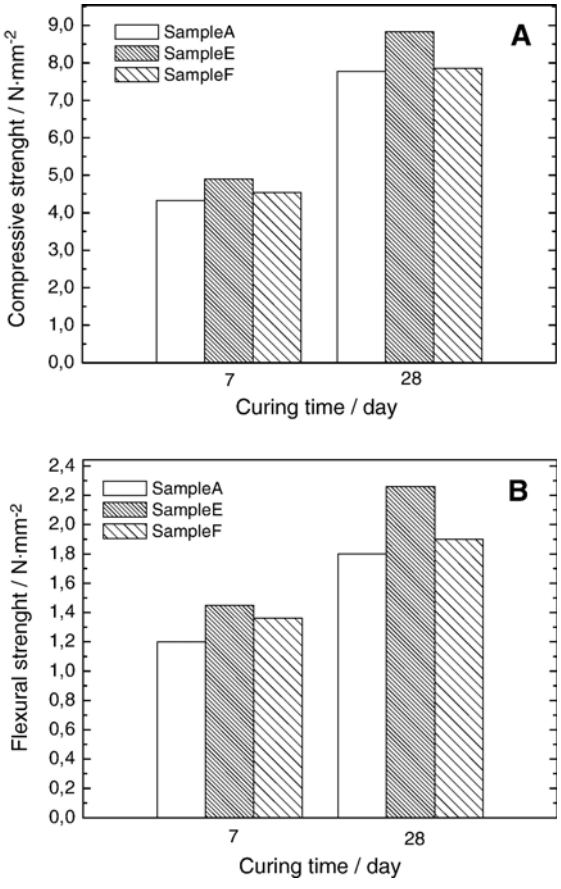

Fig. 8. (A) Compressive and (B) flexural strength as a function of curing time in mortars prepared by decreasing the cement/limestone ratio.

The pore structure was examined in order to confirm some of the previous assumptions. As previously reported, porosity influences the strength of cement-based mortars [8,14,15]. Fig. 7 shows the pore size distribution of samples A and D after 28 days of curing. Pore diameter fell in the 0.08−1.0 μm range, consistent with reported values for mortars of similar composition [8]. The small amount of cement present in the samples is consistent with the low proportion of pores less than 80 nm in diameter, the origin of which is usually ascribed to the gel and capillary pores of CSH structure [10,16]. Sample A exhibited a somewhat wider pore diameter range and contained a significant proportion of pores larger than 1 μm. The presence of large pores can be due to poor cohesion between the binder and aggregate [7]. These pores were found to detract from the mechanical properties and combined with the chemical reactions involved in the setting of mortar to produce the lowest strength values measured. By contrast, the fraction of large pores is markedly decreased in sample D, probably as a result of the disparate morphology of its limestone particles. The fibre-like morphology of such particles may facilitate the formation of a stronger framework where the smaller needles of calcium silicate hydrates might fill the spaces between aggregate particles. This microstructure is consistent with the improved strength observed in sample D.

Finally, we studied two mortars that were prepared by using mussel shells alone as limestone aggregate and replacing a small fraction of the cement with the biological limestone (samples E and F). Their compositions are given in Table 1 and their compressive and flexural strength as measured after 7 and 28 days of curing shown in Fig. 8. The values for sample A are also included for comparison. The new mortars exhibited similar or even higher strength in spite of they have a lower binder/aggregate ratio. Specifically, the compressive strength of sample E was higher than that of sample A. By using m-limestone aggregate, the cement content can thus be reduced by 10% without altering the mechanical properties of the mortar, which provides a way to reduce production costs as cement is the most expensive component of mortar.

4. Conclusions

Limestone obtained as a by-product from waste of the mussel cannery industry is an effective choice for use as aggregate in mortar with improved mechanical properties relative to quarry limestone. The presence of a significant fraction of large elongated particles in the former type limestone, rather than the more rounded particles of q-limestone, facilitates the formation of a reticulate network that is a more efficient host for the fine needles of calcium silicate hydrate formed during the setting of cement. Mercury porosimetry revealed the presence of smaller pores in the mussel limestone-based mortars, consistent with more efficient filling of the pores and responsible for the increased compressive and textural strength observed. Thermogravimetric data were consistent with an improved kinetics of cement hydration and portlandite carbonation as the mussel limestone content in the mortar was increased. Finally, enhanced mechanical properties were also obtained by replacing part of cement with this limestone. This allows the formulation of new mortars with lower binder/aggregate ratios. Therefore, the use of the limestone by-product from the cannery industry to produce mortar has the following advantages: (i) it provides a new way to manage this industrial waste; (ii) it reduces mortar production costs; and (iii) it is beneficial for the environment as it reduces the need to exploit new quarries.

Acknowledgements

This work was funded by Junta de Andalucía (Group FQM-175) and the firm CEMKOSA (Project "*Caracterización Analítica, Morfológica y Estructural de Morteros de Construcción. Desarrollo de Productos Adecuados Destinados a la Construcción, Rehabilitación y Restauración de Edificios y Monumentos Históricos y Contemporáneos*").

References

[1] R. Bayer, H. Lutz, Dry Mortars, Ullmann's Encyclopedia of Industrial Chemistry, vol. 9, Wiley−VCH, 2003.
[2] J.L. Álvarez Cabrera, F. Urrutia, D. Lecusay, A. Fernández, Morteros de albañilería con escombros de demolición, Mater. Constr. 47 (1997) 43–48.
[3] N.M. Al-Akhras, M.M. Smadi, Properties of tire rubber ash mortar, Cem. Concr. Compos. 26 (2004) 821–826.
[4] T. Cerulli, C. Pistolesi, C. Maltese, D. Salvioni, Durability of traditional plasters with respect to blast furnace slag-based plaster, Cem. Concr. Res. 33 (2003) 1375–1383.
[5] G.A. Rao, Investigations on the performance of silica fume-incorporated cement pastes and mortars, Cem. Concr. Res. 33 (2003) 1765–1770.
[6] G. Li, X. Wu, Influence of fly ash and its mean particle size on certain engineering properties of cement composite mortars, Cem. Concr. Res. 35 (2005) 1128–1134.
[7] J. Lanas, J.L. Pérez, M.A. Bello, J.I. Alvarez, Mechanical properties of natural hydraulic lime-based mortars, Cem. Concr. Res. 34 (2004) 2191–2201.
[8] J. Lanas, J.I. Alvarez, Masonry repair lime-based mortars: factors affecting the mechanical behaviour, Cem. Concr. Res. 33 (2003) 1867–1876.
[9] H.-L. Chen, Y. Tseng, K.-C. Hsu, Spent FCC catalyst as a pozzolanic material for high-performance mortars, Cem. Concr. Comp. 26 (2004) 657–664.
[10] H. Uchikawa, S. Hanehara, H. Hirao, Influence of microstructure on the physical properties of concrete prepared by substituting mineral powder for part of fine aggregate, Cem. Concr. Res. 26 (1996) 101–111.
[11] A. Bakolas, G. Biscontin, A. Moropoulou, E. Zendri, Characterization of structural byzantine mortars by thermogravimetric analysis, Thermochim. Acta 321 (1998) 151–160.
[12] J. Adams, D. Dollimore, D.L. Griffiths, Thermal analytical investigation of unaltered $Ca(OH)_2$ in dated mortars and plasters, Thermochim. Acta 324 (1998) 67–76.
[13] B. Johannesson, P. Utgenannt, Microstructural changes caused by carbonation of cement mortar, Cem. Concr. Res. 31 (2001) 925–931.
[14] M.J. Mosquera, D. Benítez, S.H. Perry, Pore structure in mortars applied to restoration. Effect on properties revelant to decay of granite buildings, Cem. Concr. Res. 32 (2002) 1883–1888.
[15] C.S. Poon, Y.L. Wong, L. Lam, The influence of different curing conditions on the pore structure and related properties of fly-ash cement pastes and mortars, Constr. Build. Mater. 11 (1997) 383–393.
[16] R.A. Cook, K.C. Hover, Mercury porosimetry of hardened cement pastes, Cem. Concr. Res. 29 (1999) 933–943.